HHS Public Access

Author manuscript

J Control Release. Author manuscript; available in PMC 2016 April 28.

Published in final edited form as:

J Control Release. 2015 April 28; 204: 70–77. doi:10.1016/j.jconrel.2015.03.001.

Evaluation of drug loading, pharmacokinetic behavior, and toxicity of a cisplatin-containing hydrogel nanoparticle

Marc P. Kai[a], **Amanda W. Keeler**[b], **Jillian L. Perry**[c], **Kevin G. Reuter**[d], **J. Christopher Luft**[b], **Sara K. O'Neal**[b], **William C. Zamboni**[b], and **Joseph M. DeSimone**[a,c,d]

Marc P. Kai: mpkai@ncsu.edu; Joseph M. DeSimone: desimone@unc.edu

[a]Department of Chemical and Biomolecular Engineering, North Carolina State University, 911 Partners Way, Raleigh, NC 27599, USA

[b]Eshelman School of Pharmacy, University of North Carolina at Chapel Hill, 257 Caudill Lab, Chapel Hill, NC 27599, USA

[c]Lineberger Comprehensive Cancer Center, University of North Carolina at Chapel Hill, 257 Caudill Lab, Chapel Hill, NC 27599, USA

[d]Department of Chemistry, University of North Carolina at Chapel Hill, 257 Caudill Lab, Chapel Hill, NC 27599, USA

Abstract

Cisplatin is a cytotoxic drug used as a first-line therapy for a wide variety of cancers. However, significant renal and neurological toxicities limits it clinical use. It has been documented that drug toxicities can be mitigated through nanoparticle formulation, while simultaneously increasing tumor accumulation through the enhanced permeation and retention effect. Circulation persistence is a key characteristic for exploiting this effect, and to that end we have developed long-circulating, PEGylated, polymeric hydrogels using the Particle Replication In Non-wetting Templates (PRINT®) platform and complexed cisplatin into the particles (PRINT-Platin). Sustained release was demonstrated, and drug loading correlated to surface PEG density. A PEG Mushroom conformation showed the best compromise between particle pharmacokinetic (PK) parameters and drug loading (16 wt %). While the PK profile of PEG Brush was superior, the loading was poor (2 wt %). Conversely, the drug loading in non-PEGylated particles was better (20 wt %), but the PK was not desirable. We also showed comparable cytotoxicity to cisplatin in several cancer cell lines (non-small cell lung, A549; ovarian, SKOV-3; breast, MDA-MB-468) and a higher MTD in mice (10 mg/kg versus 5 mg/kg). The pharmacokinetic profiles of drug in plasma, tumor, and kidney indicate improved exposure in the blood and tumor accumulation, with concurrent renal protection, when cisplatin was formulated in a nanoparticle. PK parameters were markedly improved: a 16.4-times higher area-under-the-curve (AUC), a reduction in clearance (CL) by a factor of 11.2, and a 4.20-times increase in the volume of distribution (V_d).

Correspondence to: Joseph M. DeSimone, desimone@unc.edu.

Additionally, non-small cell lung and ovarian tumor AUC was at least twice that of cisplatin in both models. These findings suggest the potential for PRINT-Platin to improve efficacy and reduce toxicity compared to current cisplatin therapies.

Keywords

Introduction

Cisplatin has played an important role as a “broad-spectrum” chemotherapeutic in the treatment of many cancers.[1] The side-effects are not trivial, however, and include significant neurological and renal toxicities, the latter being dose-limiting.[2] Incorporating the drug into a nanoparticle can increase tumor accumulation while simultaneously reducing side effects caused by systemic exposure.[3]

The key characteristic for this passive targeting of nanoparticles to tumors—an important facet of chemotherapeutic delivery—is circulation persistence. The common accepted theory of passive accretion is referred to as the enhanced permeation and retention (EPR) effect. First recognized in 1986, it was attributed to hypervasculature, enhanced permeability, and little recovery through either venous or lymphatic drainage.[4] This theory suggests that, given enough time, circulating macromolecules and nanoparticles will eventually deposit in the tumor bed. The first documented definition of EPR involved a study with proteins, but wide application to nano- and microparticles has since been explored.[5–10] In addition to selective accumulation, other advantages of nano-formulations over soluble drug include increased exposure through altered pharmacokinetics (PK), greater solubility and biocompatibility, and higher therapeutic index.[11–15]

Non-small cell lung and ovarian are two types of cancer commonly treated with cisplatin.[16] An orthotopic model of lung cancer has several advantages over a subcutaneous model. Instilling cells into the organ of origination provides the appropriate microenvironment, allowing for relevant biological interactions and implications.[17,18] Carefully specifying both the type and location of cancer increases the ability to correlate potential efficacy with particle distribution and kinetics.

Several other factors, however, also dictate the behavior of a particle once injected; these include size, elastic modulus, shape, charge, and surface chemistry (see Refs. [19–22] for comprehensive reviews). The effect of size on circulation has been well documented, and evidence has mounted in favor of particles less than 100 nm in at least one critical dimension for blood persistance.[23– 25] Particle modulus is also important for sterile filtration techniques in formulation preparation and navigating the mechanical barriers of the liver and spleen.[26–30] The role of shape has been elusive due to a shortage of methods for precise shape control. Previous studies have alluded to the effect of particle geometry, most notably studies of high-aspect ratio particles that showed increased circulation time with increasing length.[31,32] These studies have been the driving force behind utilizing worm-like particles for EPR studies, but calibration-quality fabrication of filamentous geometry and modulus is difficult.[33,34] Surface charge plays a major role in particle stability and

biological interactions; cationic particles are more toxic to red blood cells and cause platelet aggregation compared to neutral or anionic particles.[35] PEGylation, a polymer surface coating of repeating ethylene glycol units, is a common surface modification utilized to reduce protein binding (opsonization), increase hydrophilicity and stability, and extend circulation half-life.[14,36–38] Finally, the interplay between these characteristics complicates studies even further; synergistic or dysergistic effects may be difficult to observe without precise control over all variables.

Particle Replication in Non-wetting Templates (PRINT®) is a calibration-quality tool that enables complete, orthogonal control over particle characteristics.[39,40] The capacity of PRINT to independently and systematically vary parameters is a crucial advantage in determining exactly how a given variable affects nanoparticle behavior. The modulus, shape, and surface chemistry of PRINT hydrogels were previously optimized with different PEGylation conformations (non-PEGylated, PEG Mushroom, and PEG Brush).[27,41] The aim of this study was to investigate the effect of surface PEG density on the loading and release of cisplatin from nanoparticles, and subsequently determine the *in vivo* behavior of the optimal formulation. Herein we report a platform and method for novel complexation and release of cisplatin from a PRINT hydrogel nanoparticle (PRINT-Platin).

Materials and Methods

Materials

Commercially available polyethylene glycol diacrylate (PEG_{700}-DA, Mn=700 Da), 2-aminoethyl methacrylate hydrochloride (AEM), diphenyl(2,4,6-trimethylbenzoyl)-phosphine oxide (TPO), polyvinyl alcohol (PVOH, Mn=2000 Da), succinic anhydride, cis-diaminedichloroplatinum(II) (CDDP), and sucrose were purchased from Sigma-Aldrich. PTFE syringe filters (13mm membrane, 0.220 μm pore size), dimethylformamide (DMF), triethanolamine (TEA), pyridine, sterile water, borate buffer (pH 8.6), methanol, and trace-metal grade concentrated nitric acid (HNO_3) were obtained from Fisher Scientific. Methoxy PEG (5k)-succinimidyl carboxy methyl ester (mPEG5k-SCM) was purchased from Creative PEGWorks. Tetraethylene glycol monoacrylate (HP_4A) was synthesized in-house as previously described.[42] Conventional filters (2 μm) were purchased from Agilent, and polyvinyl alcohol (Mw 2000) (PVOH) was purchased from Acros Organics. PRINT molds (80 nm × 320 nm) were obtained from Liquidia Technologies (RTP, NC). Polyethylene terephthalate (PET) was purchased in 1000-foot rolls from 3M. Cisplatin was acquired from the University of North Carolina Pharmacy. Water, where used, was sterile-grade and 0.2-μm filtered. Cells (A549-luc, SKOV-3, and MDA-MB-468) were purchased from American Type Culture Collection. Fetal bovine serum was purchased from Atlanta Biologicals. RPMI 1640 Medium was purchased from Gibco®; Leibovitz's L-15 and McCoy's 5A Media were purchased from Corning cellgro®. All commercially available materials were used as received.

Fabrication, functionalization, and complexation

The PRINT particle fabrication technique has been described previously in detail.[41,43] Briefly, a preparticle solution (PPS) was prepared by dissolving various reactive monomers

in methanol. The PPS "solids" were comprised of 69 wt% HP_4A, 20 wt% AEM, 10 wt% $PEG_{700}DA$, and 1 wt% TPO. A thin film of the PPS was drawn onto PET, laminated to the patterned side of the mold, and delaminated at the laminator nip roll. Particles were cured by passing the filled mold through a UV-LED (Phoseon). A PVOH harvesting sheet was hot laminated to the filled mold and cooled to room temperature (r.t.), and particles were removed from the mold by splitting the PVOH harvesting sheet from the mold. Particles were then harvested by dissolving the PVOH in water and passed through a 2 μm filter (Agilent) to remove any large particulates. To remove the excess PVOH, particles were centrifuged (Eppendorf Centrifuge 5417R) at *ca*. 21,000 × g for 15 minutes at 4 °C, the supernatant was removed, and the particles were re-suspended in sterile water. This purification process was repeated two times in water, followed by three times in DMF, to prepare particles for PEGylation and succinylation.

The particles (1 mg/mL) were reacted with excess TEA for 10 minutes at r.t. on a shaker plate (Eppendorf, 1400 rpm). The $mPEG_{5k}$-SCM was dissolved in DMF (14 mg for PEG Brush; 2.05 mg for PEG Mushroom, previously optimized [41]; none for non-PEGylated and non-succinylated) and added to the reaction mixture. The reaction mixture was shaken overnight and quenched with borate buffer (100 μL). The nanoparticle suspension was then washed three times with DMF via centrifugation. Particles were succinylated by reaction with an excess of pyridine and succinic anhydride (100X molar excess with respect to amine groups; no succinic anhydride was added to non-succinylated particles). The reaction was carried out in a sonicator bath (Branson Ultrasonic Cleaner 1.4 A, 160 W) for 30 minutes. Following succinylation, the particles were washed by centrifugation once in DMF, followed by a borate buffer wash to neutralize any succinic acid side product, and then three washes with sterile water.

Cisplatin complexation was achieved by incubating the particles in a solution of CDDP (2X molar excess with respect to carboxyl groups) in water at r.t. for >24 hours under constant agitation (Eppendorf, 1400 rpm). After incubation in the complexation solution, particles were washed with sterile water by centrifugation and resuspended in 9.25 wt% sucrose (aq) at the appropriate dose concentration. Aliquots were flash frozen in liquid nitrogen and stored at −20 °C until needed.

Characterization

Particle concentrations were determined by thermogravimetric analysis (TGA) using a TA Instruments Q5000 analyzer. Particles were visualized via scanning electron microscopy (SEM) using a Hitachi S-4700 microscope. Prior to imaging, SEM samples were coated with 1.5 nm of gold-palladium alloy using a Cressington 108 auto sputter coater. Particle size and zeta potential were measured by dynamic light scattering (DLS) on a Zetasizer Nano ZS (Malvern Instruments, Ltd.) at 37 °C.

For release studies, PRINT-Platin was incubated at 1 mg/mL in PBS buffer on a shaker at 1400 rpm, 37 °C (n=3 per particle type). An aliquot was taken from each sample at 24, 48, 72, and 168 hours. The sample aliquot was centrifuged (*ca*. 21,000 × g, 15 minutes, 4 °C) to isolate cisplatin in the supernatant released from the particle pellet. The supernatant samples were stored before analysis.

Cisplatin loading and release were assessed using an Agilent 1200 series high-performance liquid chromatography (HPLC) system with an ultraviolet detector. The mobile phase consisted of 90 % 0.9-wt% NaCl (aq) and 10 % methanol, by volume. A five minute isocratic elution protocol was used with a ZORBAX Eclipse Plus C18 column (Agilent Technologies). The product was eluted at a flow rate of 1 mL/min and monitored at a wavelength of 210 nm. Drug loading was determined by analysis of the complexation solution pre- and post-incubation. The net difference in cisplatin concentration was calculated as weight percent in the particle.

Cytotoxicity

Cells were seeded in 200 μL of media [RMPI 1640 Medium for A549; McCoy's 5A Medium for SKOV-3; Leibovitz's L-15 Medium for MDA-MB-468; all media was supplemented with 10 % fetal bovine serum] at a density of 5000 cells per cm^2 into a 96-well microtiter plate. Cells were allowed to adhere for 24 hours and subsequently incubated with either PRINT-Platin or cisplatin at concentrations ranging from 9.8 nM to 80 μM (drug concentration) for 72 hours at 37 °C in a humidified 5 % CO_2 atmosphere. After the incubation period, all media/particles were aspirated off cells. 100 μL fresh medium was added back to cells, followed by the addition of 100 μL CellTiter-Glo® Luminescent Cell Viability Assay reagent (Promega, Madison, WI). Plates were placed on a microplate shaker for 2 minutes, then incubated at r.t. for 10 minutes to stabilize luminescent signal. The luminescent signal was recorded on a Molecular Dynamics SpectraMax M5 plate reader. The viability of the cells was expressed as a percentage of the viability of cells grown in the absence of particles or drug.

Animals

All experiments involving mice were performed in accordance with the National Research Council's Guide to Care and Use of Laboratory Animals (1996), under an animal use protocol approved by the University of North Carolina Animal Care and Use Committee. All studies used female Foxn1nu (athymic nude, C57BL/6J background) mice (5 weeks old, 17–27 g, Jackson Laboratory). For the tumor accumulation PK study, an orthotopic non-small cell lung (A549-luc) model and a subcutaneous ovarian (SKOV-3) model were used. Cell cultures were prepared and maintained per vendor specifications. For the orthotopic lung model, a 40-μL suspension of luciferase-expressing A549 cells (5×10^6 cells per mouse in a 50:50 Matrigel:PBS blend) was implanted into the lung via intra-thoracic inoculations, as previously described.[18] For the subcutaneous ovarian model, a 200-μL suspension of SKOV-3 cells (5×10^6 cells per mouse in a 50:50 Matrigel:PBS blend) was injected into the left flank of the mice. Tumor growth was monitored by bioluminescence (A549) or volume (SKOV3) via caliper measurements ($L^2 \times W/2$).

Pharmacokinetic study in healthy mice

PRINT-Platin or cisplatin was dosed via tail vein injections at 3 mg drug per kg of mouse weight in naïve animals based on drug amount. Nanoparticles were injected as a suspension in an isotonic sucrose solution (9.25 wt%), and cisplatin was dosed in prescription form (pH-adjusted 0.9 wt% NaCl solution). Liver, spleen, and kidney were harvested and flash-frozen in liquid nitrogen at 0.083, 0.5, 1, 6, 24, and 72 hours post-injection. Four mice per

arm were examined at each time point. Blood was collected in EDTA by cardiac puncture at the same time points and centrifuged (300 × g, 5 minutes, 4 °C) to isolate plasma from the cell fraction. A portion of the plasma samples from the soluble drug arm was set aside to separate protein-bound cisplatin from unbound cisplatin. For the separation of protein-bound cisplatin from unbound cisplatin, plasma was pipetted into a Centrifree ultracentrifugation device (EMD Millipore Co.) and centrifuged at 2500 × g for 30 minutes at 25 °C.

Pharmacokinetic analysis of the measured plasma concentrations was performed using PKSolver.[44] Data was fit to either a one- or two-compartment model, and the Akaike information criterion (AIC) was used to compare goodness of fit for each nanoparticle type.[45]

Tumor accumulation

Once tumors had reached sufficient size post-tumor inoculation, mice were randomized into dosing groups. PRINT-Platin or cisplatin was dosed via tail vein injections at the maximum tolerated dose (MTD), based on drug amount. Tumors were harvested and flash-frozen in liquid nitrogen at 0.083, 0.5, 1, 6, 24, and 72 hours post-injection. Four mice per arm were examined at each time point.

Maximum tolerated dose (MTD)

Cisplatin or PRINT-Platin (n=3) was dosed intravenously in naïve mice via tail-vein once per week for six weeks. Acceptable body weight loss was specified as ≤20 %, per protocol guidelines. Injections and animal welfare monitoring were performed with the assistance of the Animal Studies Core (UNC-CH).

ICP-MS validation, quantification, and analysis

Tissue sample preparation was performed as previously described.[46] Briefly, tissue (kidney, tumor, liver, spleen) and plasma samples were digested in concentrated HNO_3 spiked with 200 ng/mL Iridium (Ir; analytical internal standard, Inorganic Ventures, Christiansburg, VA) for 60–90 minutes at 90 °C. Deionized water was added to bring sample to volume and HNO_3 concentration of 3.5 %, and the samples were stored at 4 °C until platinum (Pt) analysis was completed. Inductively-coupled plasma mass spectroscopy (ICP-MS) analysis (Agilent 7500cx) was performed and validated as previously described.[46,47]

Results and Discussion

Characterization and drug release of calibration-quality nanoparticles

Incorporation of cisplatin into PRINT hydrogels was achieved via ligand exchange of a chloride atom on the drug with a carboxyl group within the particle matrix (Figure 1). Complexation of cisplatin into a matrix was previously shown in micelles containing aspartic acid and was demonstrated by this group using a PEG-based hydrogel.[48]

Since hydrogels swell based upon composition and conditions, it was important to monitor the particles for any changes during production. Demonstration of stability in the solid-state

form was also important for long-term storage potential. Figure 2 shows a representative comparison of SEM images and DLS measurements for purified particles after harvest and cisplatin-loaded particles that were flash frozen in sucrose. These measurements indicate that particle integrity was maintained throughout the functionalization and complexation process, with no apparent change in particle characteristics. This validation of the morphology, size, and stability provides confirmation of an effective and suitable process for formulation and storage of cisplatin-loaded, PEGylated PRINT hydrogels.

The loading and release of cisplatin as a function of surface PEG conformation was then investigated via HPLC. An inverse correlation between PEG density and drug loading was observed; cisplatin content increased as PEGylation decreased (Figure 3A). Although non-PEGylated particles afforded the highest drug loading, previous studies revealed that the *in vivo* PK was quite poor compared to PEG Brush and PEG Mushroom particles.[41] These studies showed an increase of 200-times and 136-times the clearance of PEG Brush and PEG Mushroom particles, respectively. Furthermore, the exposure (area under the curve [AUC]) was reduced by a factor of 127 and 86 over Brush and Mushroom conformations, respectively. Conversely, although the PEG Brush conformation had the best PK parameters, it had the lowest cisplatin loading. It was hypothesized that steric hindrance from the thicker PEG coating on the surface prohibited cisplatin from diffusing into the interior of the particle. The PEG Mushroom conformation offered a moderate improvement in PK parameters compared to PEG Brush and only a small decrease in cisplatin loading compared to non-PEGylated. Thus, PEG Mushroom was considered the optimal particle—hereafter referred to as PRINT-Platin—since it offered the best compromise between drug loading and circulation behavior. The release profile of cisplatin from the particles also supported this conclusion (Figure 3B). The majority of encapsulated drug was released from each particle type; demonstration of release from the carrier is vital for effective delivery. An additional negative control (non-succinylated particles) presented minimal release, which was expected since there were no carboxyl groups for cisplatin complexation.

Cytotoxicity of drug and particles on A549, SKOV-3, and MDA-MB-468

To evaluate the *in vitro* toxicity of the new formulation, we investigated the effects of PRINT-Platin on several cancer cell lines as compared to cisplatin. As discussed previously, the PEG Mushroom particle was used as it appeared to possess the appropriate balance between cisplatin content and pharmacokinetic parameters. Non-small cell lung, ovarian, and breast cancers were screened to demonstrate that particle effectiveness was independent of tumor selection. The former two diseases are approved indications of cisplatin, and the latter breast line represented potential future targets. The nanoparticle complex showed cytotoxicity in all cell lines tested, but was less toxic compared to the soluble drug (Figure 4). This was an expected shift due to the release profile of the drug from the particle matrix. Cells were exposed to particles for 72 hours, at which point approximately 60% of the encapsulated drug would have released (Figure 3B). Blank particles showed no toxicity, agreeing with previous studies on PEG-based PRINT hydrogels.[49–51]

Verification that active drug is recovered in a biological setting is paramount to continued investigations of the formulation, as several other cisplatin-nanoparticle platforms failed to

achieve results due to a lack of drug release.[52,53] Coupled with HPLC analysis, the cytotoxicity assays confirmed *in vitro* release of cisplatin from PRINT-Platin.

Pharmacokinetic study in healthy mice

In order to determine the benefits of formulating cisplatin in a nanoparticle, quantitative analysis of the drug was performed using ICP-MS. An equimolar amount of drug was injected for accurate comparison of cisplatin distribution. Figure 5 portrays the plasma kinetics and parameters of PRINT-Platin and cisplatin. Given at the same concentration, PRINT-Platin was retained in the blood at a higher concentration at all time points (Figure 5A). The pharmacokinetic (PK) parameters revealed a marked improvement in the circulation behavior of PRINT-Platin as compared to cisplatin (Figure 5B). There was a 16.4-times higher exposure, expressed as area-under-the-curve (AUC), representing a higher total amount of drug reaching circulation. A decrease in the clearance (CL) by a factor of 11.2 indicated slower removal of the drug from the body. Finally, the volume of distribution (V_d) increased by 4.20- times, which implied an apparent decrease in the amount of drug that was tissue-bound for the particulate form. Overall, the PK of cisplatin was vastly improved by the nanoparticle formulation.

Encapsulation within a vehicle is also important and affords protection of cisplatin from protein binding and inactivation. Figure 5C shows the majority of drug is retained within the particle while in circulation, potentially minimizing toxicity in non-target, healthy tissues. Finally, renal protection was demonstrated in the particle formulation. Figure 5D revealed lower kidney accumulation of PRINT-Platin compared to cisplatin. This suggests the potential for the nano-formulation to mitigate nephrotoxicity, increasing the therapeutic index to improve a patient's quality of life and increase the tolerable drug dose, with implications for better efficacy.[2,54] The pharmacokinetic profile in both liver and spleen displayed higher accumulation of PRINT-Platin compared to cisplatin (Supplemental Figure 1) as expected due to the enhanced sequestration of particles by these organs, however, no adverse toxicity was observed.

Maximum tolerated dose of drug and particles in naïve mice

The maximum tolerated dose (MTD) is also an important factor in determining the dose of a formulation and can be a predictor of clinical success.[55] It is also the first step in determining toxicity in a pre-clinical model. As shown in Figure 6, the *in vivo* toxicity of cisplatin and PRINT-Platin was determined by monitoring the body weight of mice dosed at varying levels of drug (3, 5, 6 mg/kg and 5, 10, 15 mg/kg for cisplatin and PRINT-Platin, respectively) over the course of six weekly injections. Soluble cisplatin was well-tolerated at 3 and 5 mg/kg doses for the entirety of the study. Following the fourth dose, however, all of the 6 mg/kg mice dropped below the acceptable weight loss. This was in agreement with the MTD of cisplatin from other studies, where substantial variation was shown based on dose schedule and mouse strain (ranging from 9 mg/kg for a single dose to 3–6 mg/kg for repeated doses).[16,56,57] PRINT-Platin was tolerated at higher doses than drug alone; mice dosed at 5 and 10 mg/kg equivalent drug presented minimal weight loss over the course of the six-week treatment. Other nanoparticle formulations have been shown to also have a higher MTD, as systemic exposure of drug is reduced in an encapsulated form.[58–60] The

highest dose, 15 mg/kg, was tolerated through four doses. Shortly after the fifth dose, however, all mice experienced significant weight loss, indicating significant toxicity. Finally, a blank, non-loaded particle (equivalent concentration of the highest PRINT-Platin dose) showed no decline in weight. This bolstered the *in vitro* results, providing further evidence that the carrier itself has no toxic side effects.

Tumor accumulation

A study to measure the tumor delivery of cisplatin via particle or soluble form was undertaken. The ability to selectively accumulate drug at the site of cancer can be a predictor of efficacy.[61] To that end, passive delivery of cisplatin was examined in an orthotopic model of non-small cell lung cancer and a subcutaneous model of ovarian cancer. In both non-small cell lung-derived and ovarian tumor models, a trend towards higher accumulation of PRINT-Platin over cisplatin was observed (Figure 7). Drug was dosed at the MTD of each formulation: 5 mg/kg for cisplatin and 10 mg/kg for PRINT-Platin. As expected, the data showed that tumor exposure of cisplatin delivered via PRINT-Platin was at least twice as high as the soluble form. Of interest was the 2.40-times higher AUC for PRINT-Platin in the ovarian model, indicative of an enhanced accumulation of cisplatin when delivered in particulate form. In both types of tumors, the ability to transport more drug with less kidney accumulation would result in a higher therapeutic index. This suggests the potential for PRINT-Platin to have better efficacy over cisplatin in these models.

Conclusions

Cisplatin is a potent chemotherapeutic for a wide variety of tumor models, but its dose-limiting toxicity—specifically renal failure—prevents it from being more efficacious. Furthermore, its continued use diminishes the patient's standard-of-living due to neuro- and ototoxicity. The potential benefits of formulating the drug into a nanoparticle include increased tumor accumulation, prolonged circulation, and renal protection, resulting in a remedy for many of the traditional drawbacks to prescribing cisplatin.

We demonstrated a surface PEGylation density-dependent loading of drug for PRINT hydrogel nanoparticles. For studies in a biological setting, this loading was compared to the circulation pharmacokinetic parameters to find the optimal formulation. The ability to safely deliver a larger amount of drug is promising for antitumor studies. PRINT-Platin has the potential to mitigate the dose-limiting toxicity associated with cisplatin, leading to more efficacious treatment and a higher therapeutic index. Future investigation into the *in vivo* anti-cancer effects of PRINT-Platin would reveal the potential for therapeutic applications.

Supplementary Material

Refer to Web version on PubMed Central for supplementary material.

Acknowledgements

The authors would like to thank Charlene Santos, Mark Ross, and the UNC Animal Studies Core for their support and indispensable help with the murine experiments. They also thank Dr. Stuart Dunn, Dr. Kevin Chu, Yancey Luft, and Thomas Flannery for their valuable contributions to this work, and Dr. Ashish Pandya for the synthesis of

HP4A. All authors have given approval to the final version of the manuscript. This work was supported by Liquidia Technologies and the Carolina Center for Cancer Nanotechnology Excellence (U54CA151652).

References

1. Shen D-W, Pouliot LM, Hall MD, Gottesman MM. Cisplatin resistance: a cellular self-defense mechanism resulting from multiple epigenetic and genetic changes. Pharmacol. Rev. 2012; 64:706–721. [PubMed: 22659329]
2. Yao X, Panichpisal K, Kurtzman N, Nugent K. Cisplatin nephrotoxicity: a review. Am. J. Med. Sci. 2007; 334:115–124. [PubMed: 17700201]
3. Davis ME, Chen ZG, Shin DM. Nanoparticle therapeutics: an emerging treatment modality for cancer. Nat. Rev. Drug Discov. 2008; 7:771–782. [PubMed: 18758474]
4. Matsumura Y, Maeda H. A new concept for macromolecular therapeutics in cancer chemotherapy: mechanism of tumoritropic accumulation of proteins and the antitumor agent smancs. Cancer Res. 1986; 46:6387–6392. http://www.ncbi.nlm.nih.gov/pubmed/2946403. [PubMed: 2946403]
5. Arias JL, Reddy LH, Couvreur P. Polymeric nanoparticulate system augmented the anticancer therapeutic efficacy of gemcitabine. J. Drug Target. 2009; 17:586–598. [PubMed: 19694612]
6. Hatakeyama H, Akita H, Harashima H. A multifunctional envelope type nano device (MEND) for gene delivery to tumours based on the EPR effect: a strategy for overcoming the PEG dilemma. Adv. Drug Deliv. Rev. 2011; 63:152–160. [PubMed: 20840859]
7. Li S-D, Huang L. Surface-modified LPD nanoparticles for tumor targeting. Ann. N. Y. Acad. Sci. 2006; 1082:1–8. [PubMed: 17145918]
8. Maeda H, Wu J, Sawa T, Matsumura Y, Hori K. Tumor vascular permeability and the EPR effect in macromolecular therapeutics: a review. J. Control. Release. 2000; 65:271–284. http://www.ncbi.nlm.nih.gov/pubmed/10699287. [PubMed: 10699287]
9. Tseng Y-C, Mozumdar S, Huang L. Lipid-based systemic delivery of siRNA. Adv. Drug Deliv. Rev. 2009; 61:721–731. [PubMed: 19328215]
10. van de Ven AL, Kim P, Haley O, Fakhoury JR, Adriani G, Schmulen J, et al. Rapid tumoritropic accumulation of systemically injected plateloid particles and their biodistribution. J. Control. Release. 2012; 158:148–155. [PubMed: 22062689]
11. Drummond DC, Meyer O, Hong K, Kirpotin DB, Papahadjopoulos D. Optimizing liposomes for delivery of chemotherapeutic agents to solid tumors. Pharmacol. Rev. 1999; 51:691–743. http://www.ncbi.nlm.nih.gov/pubmed/10581328. [PubMed: 10581328]
12. Gref R, Lück M, Quellec P, Marchand M, Dellacherie E, Harnisch S, et al. “Stealth” corona-core nanoparticles surface modified by polyethylene glycol (PEG): influences of the corona (PEG chain length and surface density) and of the core composition on phagocytic uptake and plasma protein adsorption. Colloids Surf. B. Biointerfaces. 2000; 18:301–313. http://www.ncbi.nlm.nih.gov/pubmed/10915952. [PubMed: 10915952]
13. Moghimi SM, Muir IS, Illum L, Davis SS, Kolb-Bachofen V. Coating particles with a block co-polymer (poloxamine-908) suppresses opsonization but permits the activity of dysopsonins in the serum. Biochim. Biophys. Acta. 1993; 1179:157–165. http://www.ncbi.nlm.nih.gov/pubmed/8218358. [PubMed: 8218358]
14. Owens DE, a Peppas N. Opsonization, biodistribution, and pharmacokinetics of polymeric nanoparticles. Int. J. Pharm. 2006; 307:93–102. [PubMed: 16303268]
15. Papahadjopoulos D, Allen TM, Gabizon A, Mayhew E, Matthay K, Huang SK, et al. Sterically stabilized liposomes: improvements in pharmacokinetics and antitumor therapeutic efficacy. Proc. Natl. Acad. Sci. U. S. A. 1991; 88:11460–11464. http://www.pubmedcentral.nih.gov/articlerender.fcgi?artid=53155&tool=pmcentrez&rendertype=abstract. [PubMed: 1763060]
16. Boulikas T, Vougiouka M. Cisplatin and platinum drugs at the molecular level. (Review). Oncol. Rep. 2003; 10:1663–1682. http://www.ncbi.nlm.nih.gov/pubmed/14534679. [PubMed: 14534679]
17. Bibby MC. Orthotopic models of cancer for preclinical drug evaluation: advantages and disadvantages. Eur. J. Cancer. 2004; 40:852–857. [PubMed: 15120041]

18. Peng L, Feng L, Yuan H, Benhabbour SR, Mumper RJ. Development of a novel orthotopic non-small cell lung cancer model and therapeutic benefit of 2'-(2-bromohexadecanoyl)-docetaxel conjugate nanoparticles. Nanomedicine. 2014:1–10.
19. Alexis F, Pridgen E, Molnar LK, Farokhzad OC. Factors affecting the clearance and biodistribution of polymeric nanoparticles. Mol. Pharm. 2008; 5:505–515. [PubMed: 18672949]
20. Moghimi SM, Hunter aC, Andresen TL. Factors controlling nanoparticle pharmacokinetics: an integrated analysis and perspective. Annu. Rev. Pharmacol. Toxicol. 2012; 52:481–503. [PubMed: 22035254]
21. Nel AE, Mädler L, Velegol D, Xia T, V Hoek EM, Somasundaran P, et al. Understanding biophysicochemical interactions at the nano-bio interface. Nat. Mater. 2009; 8:543–557. [PubMed: 19525947]
22. Vonarbourg A, Passirani C, Saulnier P, Benoit J-P. Parameters influencing the stealthiness of colloidal drug delivery systems. Biomaterials. 2006; 27:4356–4373. [PubMed: 16650890]
23. Dreher MR, Liu W, Michelich CR, Dewhirst MW, Yuan F, Chilkoti A. Tumor vascular permeability, accumulation, and penetration of macromolecular drug carriers. J. Natl. Cancer Inst. 2006; 98:335–344. [PubMed: 16507830]
24. Jain RK, Stylianopoulos T. Delivering nanomedicine to solid tumors. Nat. Rev. Clin. Oncol. 2010; 7:653–664. [PubMed: 20838415]
25. Perrault SD, Walkey C, Jennings T, Fischer HC, Chan WCW. Mediating tumor targeting efficiency of nanoparticles through design. Nano Lett. 2009; 9:1909–1915. [PubMed: 19344179]
26. Braet F, Wisse E, Bomans P, Frederik P, Geerts W, Koster A, et al. Contribution of High-Resolution Correlative Imaging Techniques in the Study of the Liver Sieve in Three-Dimensions. Microsc. Res. Tech. 2007; 242:230–242. [PubMed: 17279510]
27. Kersey FR, Merkel TJ, Perry JL, Napier ME, Desimone JM. Effect of Aspect Ratio and Deformability on Nanoparticle Extravasation through Nanopores. Langmuir. 2012
28. Mebius RE, Kraal G. Structure and function of the spleen. Nat. Rev. Immunol. 2005; 5:606–616. [PubMed: 16056254]
29. Merkel TJ, Jones SW, Herlihy KP, Kersey FR, Shields AR, Napier M, et al. Using mechanobiological mimicry of red blood cells to extend circulation times of hydrogel microparticles. Proc. Natl. Acad. Sci. U. S. A. 2011; 108:586–591. [PubMed: 21220299]
30. Venkataraman S, Hedrick JL, Ong ZY, Yang C, Ee PLR, Hammond PT, et al. The effects of polymeric nanostructure shape on drug delivery. Adv. Drug Deliv. Rev. 2011; 63:1228–1246. [PubMed: 21777633]
31. Geng Y, Dalhaimer P, Cai S, Tsai R, Tewari M, Minko T, et al. Shape effects of filaments versus spherical particles in flow and drug delivery. Nat. Nanotechnol. 2007; 2:249–255. [PubMed: 18654271]
32. Park J, Von Maltzahn G, Zhang L, Derfus AM, Simberg D, Harris TJ, et al. Systematic Surface Engineering of Magnetic Nanoworms for in vivo Tumor Targeting. Blood. 2009; 92121:694–700.
33. a Champion J, Katare YK, Mitragotri S. Particle shape: a new design parameter for micro- and nanoscale drug delivery carriers. J. Control. Release. 2007; 121:3–9. [PubMed: 17544538]
34. Decuzzi P, Godin B, Tanaka T, Lee S-Y, Chiappini C, Liu X, et al. Size and shape effects in the biodistribution of intravascularly injected particles. J. Control. Release. 2010; 141:320–327. [PubMed: 19874859]
35. Garbuzenko O, Zalipsky S, Qazen M, Barenholz Y. Electrostatics of PEGylated micelles and liposomes containing charged and neutral lipopolymers. Langmuir. 2005; 21:2560–2568. [PubMed: 15752053]
36. Jain RK. Transport of molecules, particles, and cells in solid tumors. Annu. Rev. Biomed. Eng. 1999; 1:241–263. [PubMed: 11701489]
37. Lankveld DP, Rayavarapu RG, Krystek P, Oomen AG, Verharen HW, van Leeuwen TG, et al. Blood clearance and tissue distribution of PEGylated and non-PEGylated gold nanorods after intravenous administration in rats. Nanomedicine (Lond). 2011; 6:339–349. [PubMed: 21385136]
38. Walkey CD, Olsen JB, Guo H, Emili A, Chan WCW. Nanoparticle size and surface chemistry determine serum protein adsorption and macrophage uptake. J. Am. Chem. Soc. 2012; 134:2139–2147. [PubMed: 22191645]

39. Euliss LE, a DuPont J, Gratton S, DeSimone J. Imparting size, shape, and composition control of materials for nanomedicine. Chem. Soc. Rev. 2006; 35:1095–1104. [PubMed: 17057838]
40. Rolland JP, Maynor BW, Euliss LE, Exner AE, Denison GM, DeSimone JM. Direct fabrication and harvesting of monodisperse, shape-specific nanobiomaterials. J. Am. Chem. Soc. 2005; 127:10096–10100. [PubMed: 16011375]
41. Perry JL, Reuter KG, Kai MP, Herlihy KP, Jones SW, Luft JC, Napier M, Bear JE, DeSimone JM. PEGylated PRINT Nanoparticles : The Impact of PEG Density on Protein Binding , Macrophage Association, Biodistribution, and Pharmacokinetics. Nano Lett. 2012; 12:5304–5310. [PubMed: 22920324]
42. Guzmán J, Iglesias MT, Riande E, Compañ V, Andrio A. Synthesis and polymerization of acrylic monomers with hydrophilic long side groups. Oxygen transport through water swollen membranes prepared from these polymers. Polymer (Guildf). 1997; 38:5227–5232.
43. Enlow EM, Luft JC, Napier ME, DeSimone JM. Potent engineered PLGA nanoparticles by virtue of exceptionally high chemotherapeutic loadings. Nano Lett. 2011; 11:808–813. [PubMed: 21265552]
44. Zhang Y, Huo M, Zhou J, Xie S. PKSolver: An add-in program for pharmacokinetic and pharmacodynamic data analysis in Microsoft Excel. Comput. Methods Programs Biomed. 2010; 99:306–314. [PubMed: 20176408]
45. Akaike H. A new look at the statistical model identification. IEEE Trans. Automat. Contr. 1974; 19:716–723.
46. Combest AJ, Roberts PJ, Dillon PM, Sandison K, Hanna SK, Ross C, et al. Genetically engineered cancer models, but not xenografts, faithfully predict anticancer drug exposure in melanoma tumors. Oncologist. 2012; 17:1303–1316. [PubMed: 22993143]
47. Morrison JG, White P, McDougall S, Firth JW, Woolfrey SG, a Graham M, et al. Validation of a highly sensitive ICP-MS method for the determination of platinum in biofluids: application to clinical pharmacokinetic studies with oxaliplatin. J. Pharm. Biomed. Anal. 2000; 24:1–10. http://www.ncbi.nlm.nih.gov/pubmed/11108533. [PubMed: 11108533]
48. Yokoyama M, Okano T, Sakurai Y, Suwa S, Kataoka K. Introduction of cisplatin into polymeric micelle. J. Control. Release. 1996; 39:351–356.
49. Gratton SE, Pohlhaus PD, Lee J, Guo J, Cho MJ, Desimone JM. Nanofabricated particles for engineered drug therapies: a preliminary biodistribution study of PRINT nanoparticles. J. Control. Release. 2007; 121:10–18. [PubMed: 17643544]
50. Parrott MC, Finniss M, Luft JC, Pandya A, Gullapalli A, Napier ME, et al. Incorporation and controlled release of silyl ether prodrugs from PRINT nanoparticles. J. Am. Chem. Soc. 2012; 134:7978–7982. [PubMed: 22545784]
51. Wang J, Tian S, a Petros R, Napier ME, Desimone JM. The complex role of multivalency in nanoparticles targeting the transferrin receptor for cancer therapies. J. Am. Chem. Soc. 2010; 132:11306–11313. [PubMed: 20698697]
52. Harrington KJ, Lewanski CR, Northcote AD, Whittaker J, Wellbank H, Vile RG, et al. Phase I-II study of pegylated liposomal cisplatin (SPI-077) in patients with inoperable head and neck cancer. Ann. Oncol. 2001; 12:493–496. http://www.ncbi.nlm.nih.gov/pubmed/11398881. [PubMed: 11398881]
53. Veal GJ, Griffin MJ, Price E, a Parry, Dick GS, a Little M, et al. A phase I study in paediatric patients to evaluate the safety and pharmacokinetics of SPI-77, a liposome encapsulated formulation of cisplatin. Br. J. Cancer. 2001; 84:1029–1035. [PubMed: 11308249]
54. Cornelison TL, Reed E. Nephrotoxicity and hydration management for cisplatin, carboplatin, and ormaplatin. Gynecol. Oncol. 1993; 50:147–158. [PubMed: 8375728]
55. Marshall JL. Maximum-tolerated dose, optimum biologic dose, or optimum clinical value: dosing determination of cancer therapies. J. Clin. Oncol. 2012; 30:2815–2816. [PubMed: 22753919]
56. Newman MS, Colbern GT, Working PK, Engbers C, a Amantea M. Comparative pharmacokinetics, tissue distribution, and therapeutic effectiveness of cisplatin encapsulated in long-circulating, pegylated liposomes (SPI-077) in tumor-bearing mice. Cancer Chemother. Pharmacol. 1999; 43:1–7. http://www.ncbi.nlm.nih.gov/pubmed/9923534. [PubMed: 9923534]

57. Sengupta P, Basu S, Soni S, Pandey A, Roy B, Oh MS, et al. Cholesterol-tethered platinum II-based supramolecular nanoparticle increases antitumor efficacy and reduces nephrotoxicity. Proc. Natl. Acad. Sci. U. S. A. 2012; 109:11294–11299. [PubMed: 22733767]

58. Cheng L, Jin C, Lv W, Ding Q, Han X. Developing a highly stable PLGA-mPEG nanoparticle loaded with cisplatin for chemotherapy of ovarian cancer. PLoS One. 2011; 6:e25433. [PubMed: 21966528]

59. Devarajan P, Tarabishi R, Mishra J, Ma Q, Kourvetaris A, Vougiouka M, et al. Low renal toxicity of lipoplatin compared to cisplatin in animals. Anticancer Res. 2004; 24:2193–2200. http://www.ncbi.nlm.nih.gov/pubmed/15330160. [PubMed: 15330160]

60. Nishiyama N, Okazaki S, Cabral H, Miyamoto M, Kato Y, Sugiyama Y, et al. Novel cisplatin-incorporated polymeric micelles can eradicate solid tumors in mice. Cancer Res. 2003; 63:8977–8983. http://www.ncbi.nlm.nih.gov/pubmed/14695216. [PubMed: 14695216]

61. MacEwan SR, Callahan DJ, Chilkoti A. Stimulus-responsive macromolecules and nanoparticles for cancer drug delivery. Nanomedicine (Lond). 2010; 5:793–806. [PubMed: 20662649]

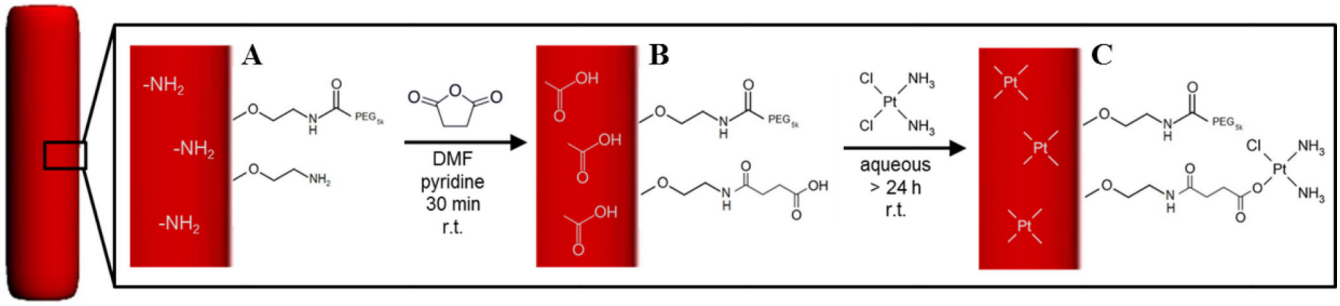

Figure 1.

Nanoparticle-cisplatin complexation schematic. The particle (red) was PEGylated and contained excess amines (**A**). The amines were converted to carboxyl groups by succinylation (**B**), which complex with cisplatin via ligand exchange with a chlorine atom (**C**).

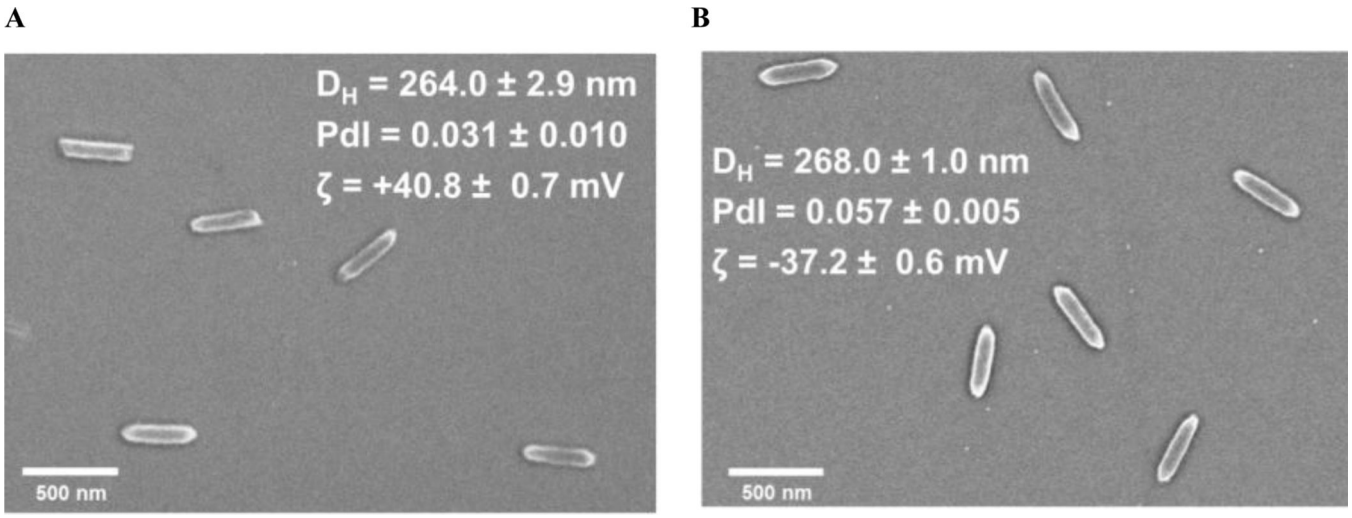

Figure 2.

SEM micrograph and dynamic light scattering data for (**A**) bare (not functionalized) 80 nm × 320 nm PRINT hydrogels and (**B**) cisplatin-loaded, PEG mushroom 80 nm × 320 nm PRINT hydrogels.

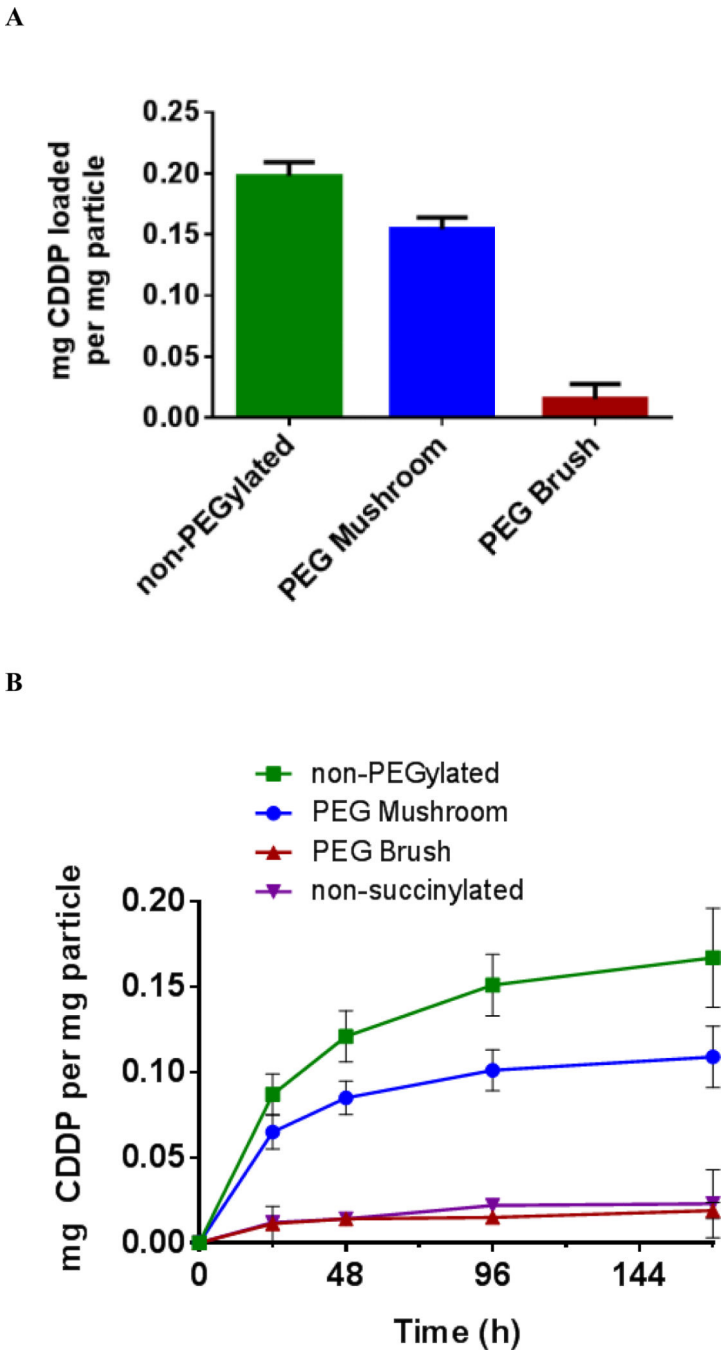

Figure 3.

Loading (**A**) and release profile (**B**) of cisplatin from 80 nm × 320 nm PRINT hydrogels as a function of surface PEG conformation in PBS at 37 °C.

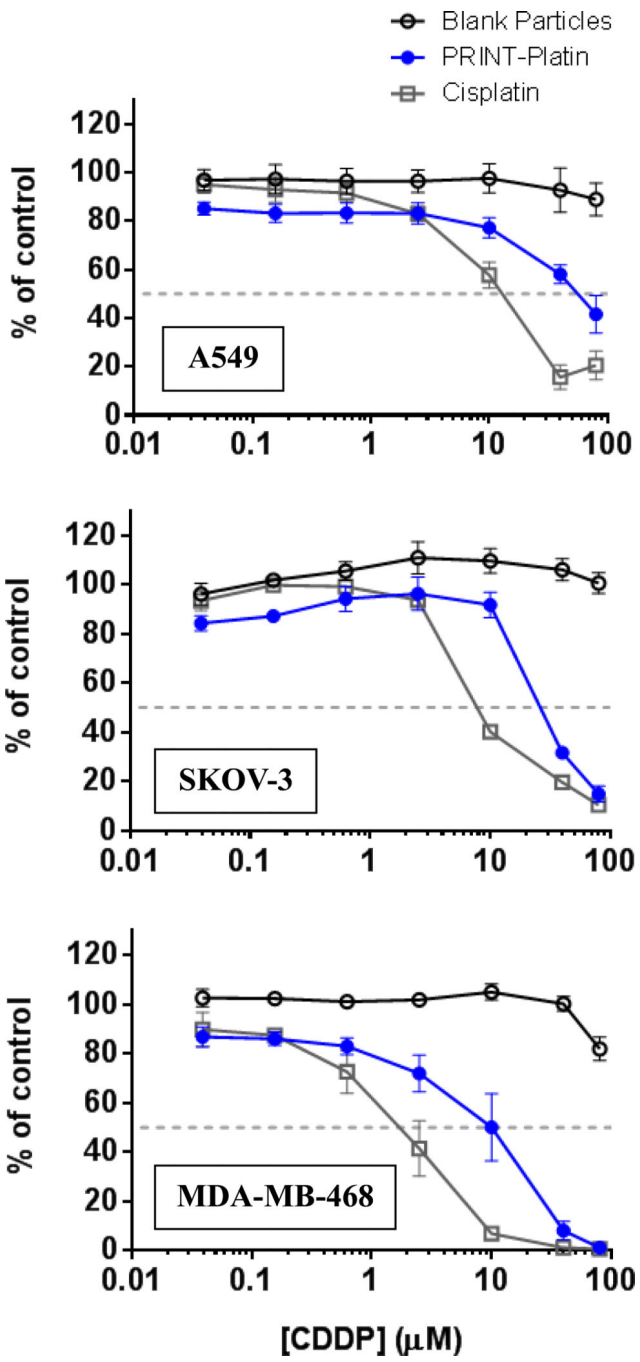

Figure 4.

Cytotoxicity of cisplatin, cisplatin-loaded 80 nm × 320 nm PEG mushroom hydrogels, and blank 80 nm × 320 nm hydrogels (no drug) in cell lines of interest: A549 (non-small cell lung), SKOV-3 (ovarian), and MDA-MB-468 (HER2-enriched breast).

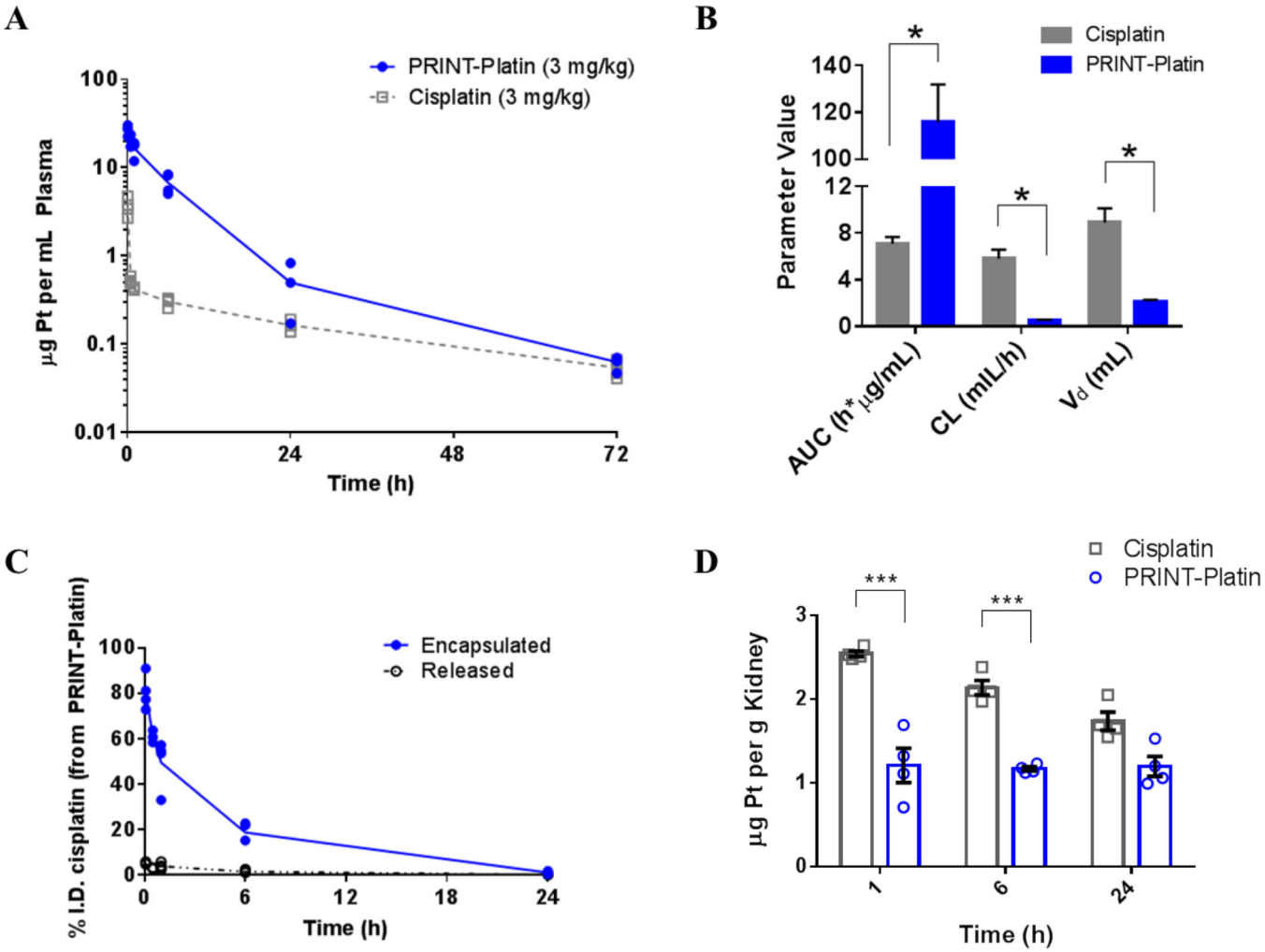

Figure 5.

Cisplatin and PRINT-Platin circulation behavior in plasma measured by inductively-coupled plasma mass spectroscopy. The plasma profile (**A**) and pharmacokinetic parameters (**B**) of cisplatin were significantly improved in particle form compared to soluble drug (* = $p < 0.05$; one-way ANOVA). Particle-bound versus released cisplatin in plasma over time (**C**) shows less than 10% of drug is released from particle while in circulation. Accumulation of platinum in kidney (**D**) shows higher levels of drug for cisplatin compared to PRINT-Platin, suggesting renal protection.

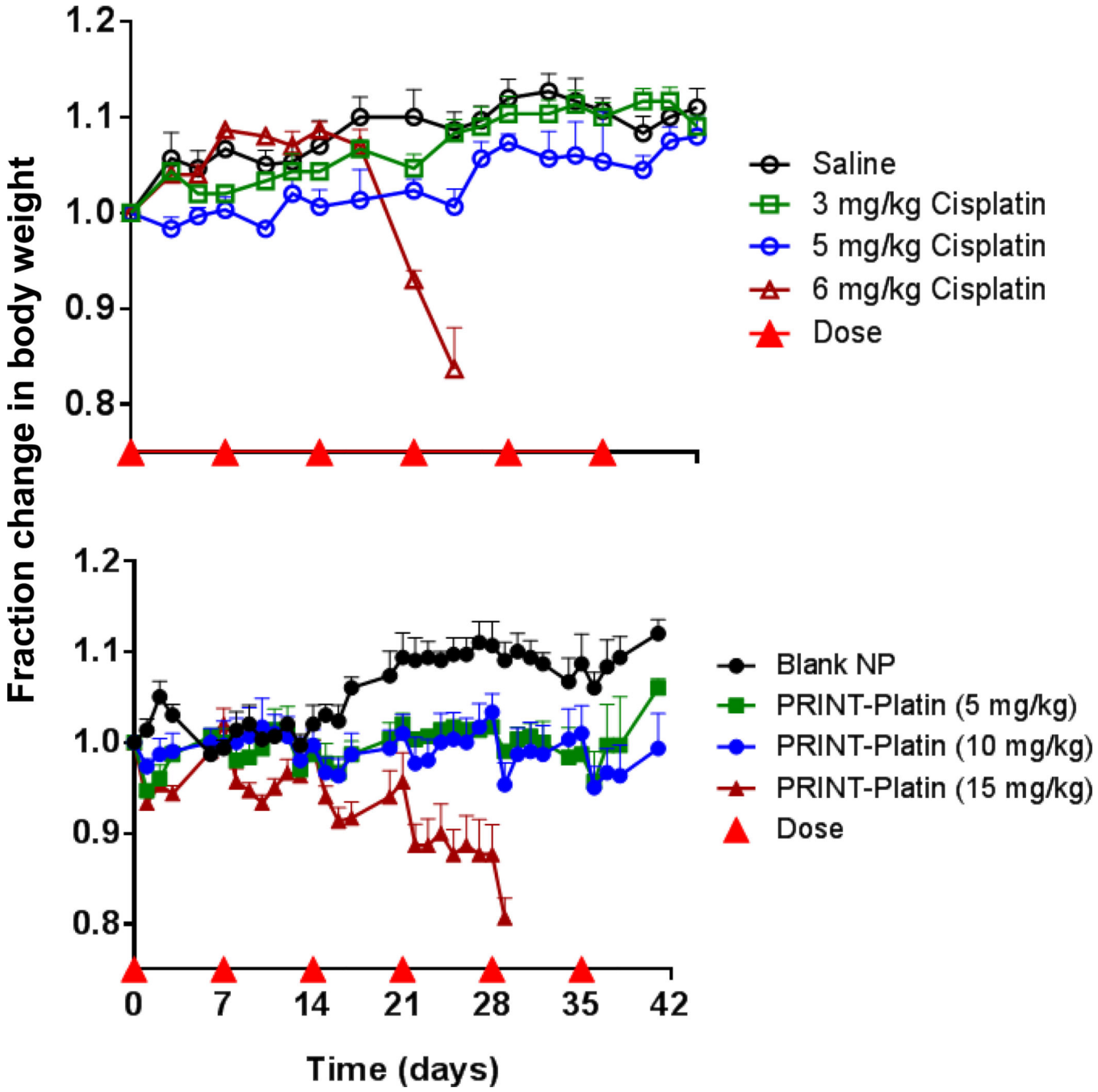

Figure 6.

Change in body weight of nude mice dosed with cisplatin, saline, PRINT-Platin (dose based on cisplatin loading), and blank PRINT nanoparticles (same particle concentration as 15 mg/kg PRINT-Platin).

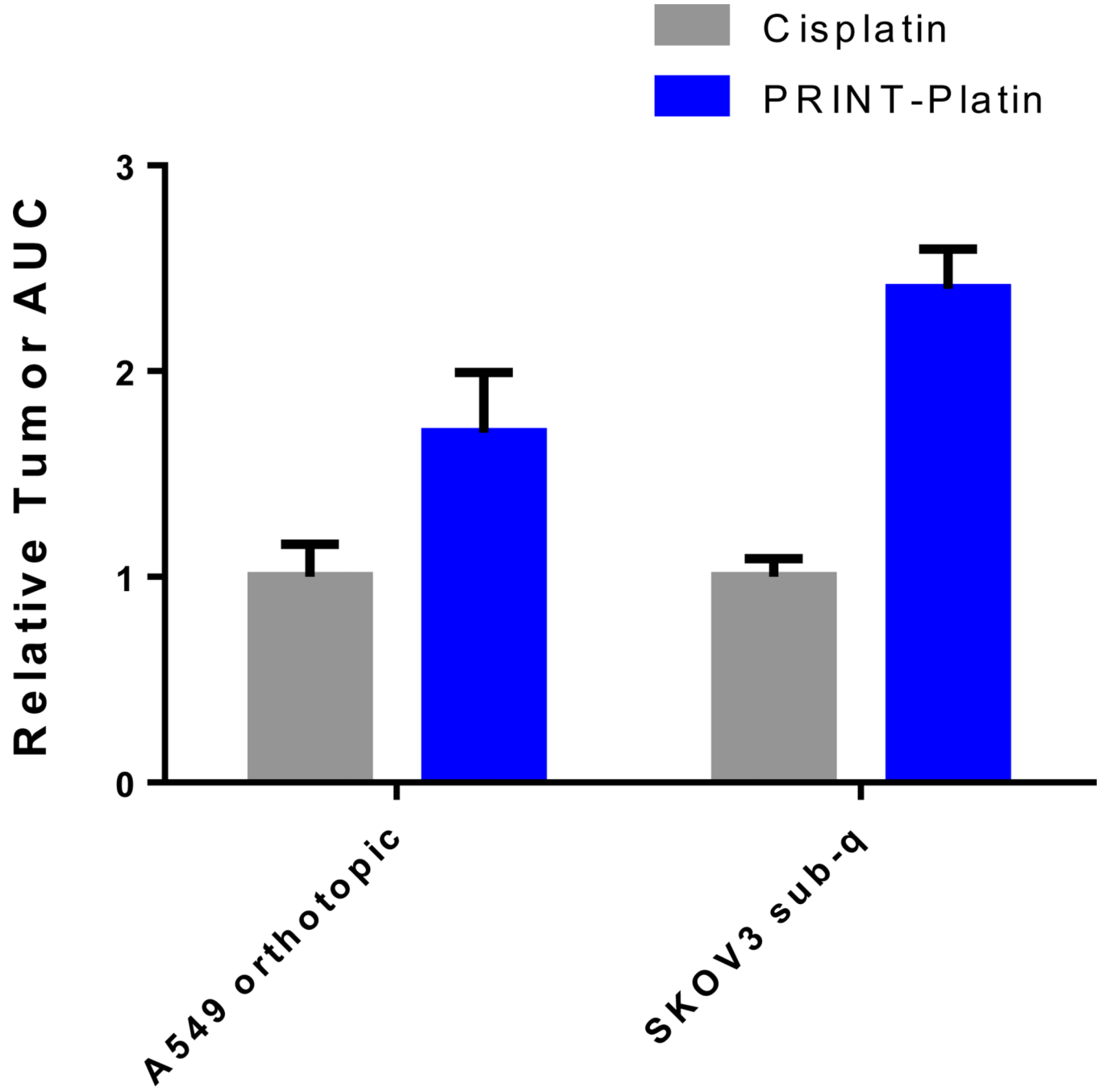

Figure 7.
Relative exposure of cisplatin versus PRINT-Platin in two tumor models measured by inductively-coupled plasma mass spectroscopy. (sub-q = subcutaneous)